Interaction between induced and natural variation at *oil yellow1* delays flowering in maize

Rajdeep S. Khangura[†§‡], Bala P. Venkata[†2], Sandeep R. Marla[†1], Michael V. Mickelbart[†‡], Singha Dhungana[3], David M. Braun[3], Brian P. Dilkes[§‡], Gurmukh S. Johal[†‡]

[†]Department of Botany and Plant Pathology, Purdue University, West Lafayette, Indiana 47907

[‡]Center for Plant Biology, Purdue University, West Lafayette, Indiana 47907

[§]Department of Biochemistry, Purdue University, West Lafayette, Indiana 47907

[3]Division of Biological Sciences, Interdisciplinary Plant Group, Missouri Maize Center, University of Missouri, Columbia, Missouri 65211

Current address

[1]Department of Agronomy, Kansas State University, Manhattan, Kansas 66506

[2]Donald Danforth Plant Science Center, St. Louis, Missouri 63132

Corresponding Authors

Brian P. Dilkes, 170 S. University Street, Purdue University, West Lafayette, Indiana 47907, Phone: (765) 494 2584, Email: bdilkes@purdue.edu

Gurmukh S. Johal, 915 W. State Street, Purdue University, West Lafayette, Indiana 47907, Phone: (765) 494-4448, Email: gjohal@purdue.edu

Author Contributions: R.S.K., B.P.V., and S.R.M. created the hybrid mapping populations; S.D. and D.M.B. performed sugar profiling; M.V.M. assisted with gas-exchange measurements; G.S.J. and B.P.D. supervised the experiments; R.S.K. and B.P.D. analyzed the data; B.P.D. and R.S.K. wrote the article with contributions of all the authors.

One-sentence summary: Natural variation in maize at chlorophyll biosynthesis gene affects flowering time through interaction with induced mutation at the same locus.

Abstract

We previously demonstrated that maize locus *very oil yellow1 (vey1)* encodes a putative cis-regulatory expression polymorphism at the magnesium chelatase subunit I gene (aka *oil yellow1*) that strongly modifies the chlorophyll content of the dominant *Oy1-N1989* mutants. The *vey1* allele of Mo17 inbred line reduces chlorophyll content in the mutants leading to reduced photosynthetic output. *Oy1-N1989* mutants in B73 flowered four days later than wild type. Enhancement of *Oy1-N1989* by the Mo17 allele at the *vey1* QTL delayed flowering further, resulting in detection of a flowering time QTL in two bi-parental mapping populations crossed to *Oy1-N1989*. The near isogenic lines of B73 harboring the *vey1* allele from Mo17 delayed flowering of *Oy1-N1989* mutants by twelve days. Just as previously observed for chlorophyll content, *vey1* had no effect on flowering time in the absence of the *Oy1-N1989* allele. Loss of chlorophyll biosynthesis in *Oy1-N1989* mutants and enhancement by *vey1* reduced CO_2 assimilation. We attempted to separate the effects of photosynthesis on the induction of flowering from a possible impact of chlorophyll metabolites and retrograde signaling by manually reducing leaf area. Removal of leaves, independent of the *Oy1-N1989* mutant, delayed flowering but surprisingly reduced chlorophyll contents of emerging leaves. Thus, defoliation did not completely separate the identity of the signal(s) that regulates flowering time from changes in chlorophyll content in the foliage. These findings illustrate the necessity to explore the linkage between metabolism and the mechanisms that connect it to flowering time regulation.

Introduction

As sexual reproduction is necessary for the production of seeds and fruits, the onset of flowering in angiosperms has been a key focus for plant biologists working on ornamental, horticultural, and other crop species (Lang 1952; Zeevaart 1962; Searle 1965). The onset of reproductive development in angiosperms is affected by a change in meristem identity. The vegetative to floral transition of meristems commits plant development to production of floral organs and sexual reproduction. The integration of signals to correctly time this transition is key to plant fitness. Unsurprisingly, endogenous and environmental cues regulate flowering time (Amasino and Michaels 2010; Cho *et al.* 2017; Minow *et al.* 2018). A critical environmental cue is the duration of the light period, or photoperiod. The photoperiodic responses of plants influence the vegetative to floral transition and the mechanisms of this response have been a focus of intensive research for over a century (Klebs, 1918). Multiple non-photoperiodic cues as well as endogenous signals, sometimes called the autonomous pathway, are also critical to floral transition. Endogenous signals including hormones and the carbon status of the plant can also play a critical role in the regulation of flowering time (Corbesier *et al.* 1998; Moghaddam and Ende 2013). But environmental influences, such as light quality, alter hormone biosynthesis (Lang 1957; Evans and Poethig 1995; Mutasa-Göttgens and Hedden 2009), and light intensity dramatically influences photosynthesis and thereby carbon status (Chen *et al.* 2004). These stimuli converge through the same floral integrators (named FLOWERING LOCUS T (FT) and FLOWERING LOCUS D (FD) in *Arabidopsis thaliana)* for which orthologs have been identified in many flowering plants (Abe *et al.* 2005; Wigge *et al.* 2005; Corbesier *et al.* 2007; Meng *et al.* 2011; Zhang *et al.* 2016). Accumulation of FT and FD gene products trigger the vegetative shoot apical meristems to acquire the competency to become inflorescence meristems and produce flowers in part via the activation of MADS-box transcription factors that control

meristem identity through APETALA1 (Abe *et al.* 2005; Wigge *et al.* 2005). In Arabidopsis, FT is regulated by CONSTANS (CO) in response to both circadian regulation and photoperiodic responses. CONSTANS itself is regulated by the MADS-box transcription factor SUPPRESSOR OF CONSTANS1 (SOC1) (Samach *et al.* 2000).

Maize was domesticated from teosinte (*Zea mays* ssp. *parviglumis* or spp. *mexicana*) in Central America (Doebley *et al.* 1997; Wang *et al.* 1999). Strong selection on time to flower contributed to the adaptation of maize to different latitudes (Salvi *et al.* 2007; Huang *et al.* 2017; Swarts *et al.* 2017). Flowering of teosinte is promoted by short-day conditions. In contrast, temperate maize germplasm is relatively day-neutral and flowering is primarily under the control of the autonomous pathway (Coles *et al.* 2010). Several mutant and QTL studies have identified loci affecting flowering time in maize (Buckler *et al.* 2009; Coles *et al.* 2010; Steinhoff *et al.* 2012; Bouchet *et al.* 2017). Some of these loci include: *indeterminate1* (*id1*; Colasanti et al. 1998); *early phase change* (*epc*; Vega et al. 2002); the maize FLORICAULA/LEAFY orthologs *zfl1* and *zfl2* (Bomblies et al. 2003); *delayed flowering1* (*dlf1*; Muszynski et al. 2006); the cis-element polymorphism *vegetative transitioning1* (*vgt1*; Salvi et al. 2007) that regulates a downstream APETALA2-like transcription factor *zmrap2.7*; *zea mays mads4* (*zmm4*; Danilevskaya et al. 2008); *zmcct10* (Hung *et al.* 2012); *zea mays centroradiales8* (*zcn8*; Meng et al. 2011); *zea mays mads1* (*zmmads1*; Alter et al. 2016); and *zea mays mads69* (Liang *et al.* 2019). Many of these encode the maize orthologs of genes identified as regulators of flowering in Arabidopsis. For example, *dlf1* and *zcn8* encode homologs of the Arabidopsis flowering time determinants FD and FT, respectively. *id1* encodes a zinc-finger transcription factor acting upstream of both DLF1 and ZCN8 (Kozaki *et al.* 2004; Muszynski *et al.* 2006; Meng *et al.* 2011). *zmm4* is an activator of flowering that is part of a conserved syntenic pair of MADS box genes in

the grasses, with *zmm24* as the neighboring gene, and encodes one of two maize paralogs of the wheat flowering time and vernalization response locus VRN1 (Danilevskaya *et al*. 2008). *zmm4* acts downstream of *dlf1* and *id1* in the control of flowering time in maize. *zmmads1* is a functional homolog of the Arabidopsis flowering time and circadian rhythm regulator *soc1* (Alter *et al.* 2016).

One important endogenous signal that contributes to flowering time is the carbon allocation status (Ohto *et al.* 2001; Seo *et al.* 2011; Eveland and Jackson 2012; Wahl *et al.* 2013; Cho *et al.* 2018). Starchless mutants of Arabidopsis exhibit delayed flowering (Corbesier *et al*. 1998). Trehalose-6-phosphate (T6P) has been implicated as a reporter of the energy status that alters flowering time in Arabidopsis (Paul 2008; Wahl et al. 2013; Seo et al. 2011). T6P and sucrose are positively correlated, and low levels of T6P results in delayed flowering in Arabidopsis (Wahl *et al*. 2013). In maize, mutants of *tie-dyed1* (*tdy1*), *tie-dyed2* (*tdy2*), *sucrose export defective1* (*sxd1*), *psychedelic (psc),* and *sucrose trasporter1* (*sut1*) that are compromised in either sugar export from source tissues or loading sucrose into the phloem also display late flowering phenotypes (Braun *et al.* 2006; Baker and Braun 2008; Ma *et al*. 2008; Slewinski *et al.* 2009; Slewinski and Braun 2010). Remarkably, the linkage between carbon status and regulation of FT/ZCN and FD/DLF1 gene products in maize may be direct. The *id1* flowering time mutants alter carbon partitioning in leaves and accumulate sucrose and starch (Coneva et al. 2012). As a result, ID1 has been proposed as a sensor of carbon status that promotes flowering (Coneva, Zhu, and Colasanti 2007; Minow et al. 2018). Interestingly, the T6P biosynthetic gene TPS1 is predicted to be a direct target of the ID1 DNA-binding protein. Consistent with this prediction, low levels of T6P were observed in maize *id1* mutants (Minow *et al.* 2018).

If sugars are critical for floral transitioning in plants, then manipulation of photosynthesis should alter flowering. Magnesium chelatase (MgChl) is a hetero-oligomeric enzyme complex that catalyzes the first committed step of chlorophyll biosynthesis by conversion of protoporphyrin IX (PPIX) into magnesium-PPIX (Walker and Weinstein 1991; Gibson et al. 1995). We previously identified a cis-acting expression polymorphism at the *oil yellow1* (*oy1)* locus (Sawers *et al.* 2006) associated with a QTL called *very oil yellow1* (*vey1*) that modifies the chlorophyll content of semi-dominant *Oy1-N1989* mutants (Khangura *et al.* 2019). We made use of these induced and natural variants to observe flowering time across material with differing photosynthetic rates and chlorophyll contents. We observed that *Oy1-N1989* mutants flowered later and that the reduced chlorophyll accumulation is associated with a delay in flowering time. Partial rescue of chlorophyll accumulation in the *Oy1-N1989* mutant phenotype by the *vey1* QTL accelerated flowering in the mutants but had no effect on wild-type siblings. These changes in chlorophyll accumulation resulted in changes in net CO_2 assimilation and photosynthetically-fixed carbon accumulation. In addition to a flowering delay, the leaf senescence induced leaf sugar accumulation following sink removal was also affected by *Oy1-N1989* and *vey1*. Suppression of photosynthate accumulation by mechanical removal of leaves, to reduce plant leaf area, also delayed flowering time. All of our results are consistent with an integrative measure of carbon assimilation linking energy status and flowering time in maize. However, every modification of carbon assimilation resulted from, or resulted in, a change in chlorophyll accumulation. This leaves unresolved whether signaling via a chlorophyll metabolite, carbon status signaling, or photosynthesis itself is responsible for this variation in flowering time.

Materials and Methods

Plant materials

The origin of *Oy1-N1989* mutant allele has been previously described (Khangura *et al.* 2019). The mutant allele is maintained in B73 background and is propagated by crossing heterozygous mutants (*Oy1-N1989/oy1*) to the wild-type siblings. The introgressed stock of *Oy1-N1989* into B73 was used for crossing to various mapping populations. A total of 216 intermated B73 × Mo17 population (IBM-RILs), and 251 synthetic 10 doubled haploid lines (Syn10-DH) were crossed as ear-parents with *Oy1-N1989/oy1*:B73 pollen. The pollen of *Oy1-N1989/oy1*:B73 plants were also crossed on to the ears of 35 B73-Mo17 near-isogenic lines (BM-NILs) for QTL validation. Tables S1-S3 contain the full list of IBM-RILs, Syn10-DH, and BM-NILs used to develop F_1 hybrid populations.

Field trials

The field experiments were conducted at the Purdue Agronomy Center for Research and Education (ACRE) in West Lafayette, Indiana. Each cross was evaluated as a single plot of 12-16 plants. Each plot derived from crosses with *Oy1-N1989/oy1*:B73 tester segregated for both mutant and wild-type siblings in approximately 1:1 ratio. Seeds were sown with tractor-driven seed planter with plot length of 3.84 meters (m) with alley length of 0.79 m, and inter-row spacing of 0.79 m. Rainfall was sufficient throughout the growing season and eliminated any need of irrigation. Standard crop management practices at Purdue in terms of fertilizer, pest, and weed control for growing field maize were adopted.

Each experiment was divided into blocks. Progenies of crosses of B73 and Mo17 ears to *Oy1-N1989/oy1*:B73 pollen were used as parental checks in each block. Parental checks were

randomized with each block. The IBM-RILs F_1 populations were evaluated as a single replication in 2013. Syn10-DH F_1 populations were evaluated in 2016 with two randomized replications planted in randomized complete block design (RCBD). Hybrid progenies of *Oy1-N1989/oy1*:B73 with BM-NILs were screened in 2016 with five replications planted in RCBD.

Field phenotyping and data collection

The mutant plants in each plot were identified visually as pale plants. The chlorophyll content in mutant and wild-type plants was approximated using a CCM-200 plus (Opti-Sciences Inc., Hudson, NH) as described in Khangura *et al.* 2019. We previously demonstrated correlation of 0.94 between CCM-200 plus values and chlorophyll *a*, chlorophyll *b*, and total chlorophyll contents (Khangura *et al.* 2019), and therefore used CCM-200 plus values (CCM) as a proxy for chlorophyll content in the materials described here. CCMI refers to measurements taken with CCM-200 plus instrument from 25-30 days after sowing and CCMII refers to measurements taken 45-50 days after sowing. Mutants were tagged around V5-V7 stages of development. Tagging is necessary as suppression of the *Oy1-N1989* mutant phenotype by *vey1* interferes with visual classification of mutant and wild-type siblings at maturity. Flowering time in each F_1 population was recorded separately on the wild-type and mutant plants. The date at which roughly half of the wild-type or mutant plants in a given plot were shedding pollen was recorded as the date of anthesis for a given genotype in that plot. Similarly, the date at which half of the wild-type or mutant plants had emerging silks was recorded as the date of silking for the respective genotype in that plot. The dates of anthesis and silking for both wild-type and mutant genotypes were then subtracted from the date of planting to obtain respective wild-type or mutant days to anthesis (DTA), and days to silking (DTS). Further, the difference between DTA and DTS was used to derive the anthesis-silking interval (ASI); ASI = DTA-DTS. Wild-type and

mutant traits are denoted with a prefix WT and MT, respectively. Ratio and differences of these flowering times values were also calculated as MT/WT and WT-MT, respectively.

Induced leaf senescence assay: A total of 15 F_1 populations derived from B73-like NILs × *Oy1-N1989/oy1*:B73 cross were used for this experiment. Seven of these B73-like NILs carried an introgression of *vey1* from Mo17 ($vey1^{Mo17}$), whereas the other eight NILs had the B73 genotype at *vey1* ($vey1^{B73}$). These NIL populations were planted in the field with at least two replications of each genotype planted in RCBD. The procedure for this experiment was adapted from Sekhon *et al.* 2012. Briefly, for the suppressing NIL, F_1 crosses of primary and secondary ears of both wild-type and mutant plants were covered with shoot bags before silk emergence. After 3-4 days of tassel shedding, roughly half of the shoot bags were removed, and these ears were allowed to open pollinate. Staggered rows of B73 were planted on both sides of the experimental row in the field to ensure pollination of exposed ears. The day of shoot exposure was marked as 0 days after anthesis (DAA). For the enhancing B73 NILs, a late set of suppressed NIL F_1 was used as a control. A similar strategy of shoot bagging of ears before silk emergence and ear exposure after 3-4 days of tassel shedding was done. The plants that showed tassel maturity on the same day were tagged and subsequently used for observation.

Genotypic and gene expression data

The genotypic data and other public datasets on various mapping populations used in this study have been described previously (Khangura *et al.* 2019). Briefly, the public marker dataset for IBM-RILs was obtained from MaizeGDB with 2,178 markers (Sen *et al.* 2010). The markers were reduced to 2,156 after removing duplicate variants, with ~13.3 percent of missing data in the final dataset. Expression data of *oy1* locus in IBM-RILs were obtained from a public repository of the National Science Foundation grant (GEPR: Genomic Analyses of shoot

meristem function in maize; NSF DBI-0820610; https://ftp.maizegdb.org/MaizeGDB/FTP/shoot_apical_meristem_data_scanlon_lab/). This data consists of the expression of maize genes in the tissue derived from the shoot apex of 14 days old IBM-RILs seedlings. The expression data from each gene is normalized to reads per kilobase of transcript per million mapped reads (RPKM). Genotypic data consisting of 6611 SNPs for Syn10-DH lines was obtained from Liu et al. 2015. This dataset had no missing genotypes and was used as such for QTL analyses. Genotypes of the B73-Mo17 Near Isogenic Lines (BM-NILs) used for QTL validation were obtained from Eichten *et al*. 2011.

Molecular analyses

OY1 sequencing: The genomic DNA and cDNA preparation derived from second and third fully-expanded leaf of maize inbred lines were used to amplify the genic sequence of the *oy1* locus. The detail description of methods and primers used for PCR amplification and sequence analyses of the PCR products has been described previously (Khangura *et al.* 2019). Briefly, the PCR amplicons were sequenced using Illumina and Sanger sequencing platforms at Purdue Genomic Core Facility.

Allele-specific expression (ASE) assay: Three replications of B73-Mo17 near-isogenic lines (BM-NILs) × *Oy1-N1989/oy1*:B73 F_1 progenies were grown in the field at Purdue Agronomy Farm along with parental F_1 checks. Mutant siblings derived from four B73-like NIL crossed with *Oy1-N1989/oy1*:B73 were selected for the ASE experiment. These NILs consisted of two B73-like NILs with $vey1^{Mo17}$, and other two B73-NILs with $vey1^{B73}$ genotype. Leaf tissue was harvested from the top fully-expanded leaf at the V3 developmental stage from the mutant siblings of the four B73-like NIL F_1 plots. For each biological replicate, tissue was pooled from 4-5 seedlings to make one sample. The samples were stored at -80 ˚C until needed. The

procedure of total RNA isolation, cDNA synthesis, and the ASE assay has been described previously in detail (Khangura *et al.* 2019). Briefly, total RNA was isolated using a modified Phenol/Lithium chloride protocol (Eggermont et. al. 1996). One µg of DNase treated RNA was used to synthesize cDNA using iScriptTM Select cDNA synthesis kit (catalog#170-8896, Bio-Rad, Hercules, CA) according to the manufacturer's recommendations. The sensitivity of the ASE assay was tested using the genomic DNA control that was prepared in the ratio of 1:1 (derived from B73 × Mo17 F_1 hybrid), 1:2, and 2:1 from B73 and Mo17 DNA. PCR was conducted using the forward oligonucleotide 5'- TCACCGTCTGCAATGTCGCCGCTC -3' and reverse oligonucleotide 5'- AGTATGCCCCTGTTGGCCTTGGCG -3' under following reaction conditions with 30 cycles of polymerization (94˚C for 30s, 56˚C for 30s, 72 ˚C for 30s and final extension for 2 minutes) to amplify the targeted region of OY1. The primer pair used in this assay flanked the SNP that causes the L176F amino acid change that resulted in the *Oy1-N1989* mutant allele. PCR products were sequenced on a MiSeq instrument (Illumina, San Diego, CA) at the Purdue Genomics Core Facility. Allele count of the reads mapped to small reference sequence derived from B73 was done using the GATK packages (DePristo *et al.* 2011). Read counts derived from GATK was used to calculate allele-specific expression. As expected, control samples derived from genomic DNA displayed bias in the read counts in a DNA dosage-dependent manner. Genomic DNA derived from B73 × Mo17 F_1 hybrids resulted in roughly 1:1 read counts demonstrating no bias in the assay.

Statistical analyses

The exploratory data analysis was done using JMP 13.0 (SAS Institute Inc. 2016). Averages of various traits from line-cross populations, IBM-RILs and Syn10-DH, were subjected to QTL analyses. QTL detection was done using a single interval mapping function "scanone" in R/qtl, a

software package implemented in R (Broman *et al.* 2003; R core Team 2013). Remarkably similar results were obtained with composite interval mapping function "cim" in R/qtl (data not shown). All the QTLs reported in this study are derived from "scanone" function.

Defoliation assay

The defoliation experiments were performed using maize inbred B73, sorghum (*Sorghum bicolor*) inbred BTx623, and green foxtail (*Setaria viridis*) inbred A10.1. These experiments were conducted under the greenhouse conditions using mogul base high-pressure sodium lamps (1000 Watts) as the supplemental light source for L:D cycle of 16:8 hours, with the temperature around 28ºC (day-time) and 20ºC (night-time). The maize inbred line B73 was defoliated at V3 leaf stage. All the leaves were removed from the base, slightly above the ligule. Sorghum inbred BTx623 plants with three to four fully opened leaves (~20 days after sowing in the greenhouse) were defoliated in a similar way. All fully expanded leaves at ~15 days after planting were removed in *Setaria* plants. In addition, all tillers were also defoliated similar to the main stem in *Setaria*. The flowering time was recorded on maize as described above. For sorghum and *Setaria*, the date of head emergence on every plant was recorded, and it was deducted from the date of planting to obtain days to heading.

Non-structural carbohydrate (NSC) quantification

The soluble sugars and starch were quantified from the mutant siblings of four B73-NILs × *Oy1-N1989/oy1*:B73 F_1 population. Two of these NILs carried $vey1^{Mo17}$, while the other two had $vey1^{B73}$ genotype. Plants were grown in the field with three replications using RCBD. Top fully-expanded leaf at the V3 stage was harvested at 1:00 PM and transferred to liquid nitrogen. Leaf tissues were stored at -80°C until needed. Leaf samples were ground into a fine powder and ~100

mg of the powder was used to extract sucrose, glucose, fructose, and starch using a previously described method (Leach and Braun 2016). The quantification of these NSC was done using a method as described (Leach *et al*. 2017). Briefly, high-performance anion exchange (HPAE) chromatography (ICS-5000, Thermo-Fisher Scientific) was used to analyze the neutral fraction of the extract. The HPAE chromatography equipped with a SA10 column was maintained at 45°C. An isocratic potassium hydroxide solution (10 mmol/L) at a constant flow rate of 1.5mL/min^{-1} was used as an eluent. Quadrupole wave form as per the manufacturer's recommendation was used for detection with a disposable gold electrode maintained at 25°C. Sugar standards were used to construct a standard curve, and samples were diluted to ensure that the detected values fell within the scope of this curve.

Gas-exchange measurements

Gas-exchange measurements were taken on the field-grown plants during the summer of 2017 at the Purdue ACRE farm. The gas-exchange measurements were taken on the third leaf on plants at the V3 stage between 11 AM and 1 PM using LICOR LI-6400XT open photosynthesis system (LI-COR Inc., Lincoln, NE, USA). Four B73-NILs × *Oy1-N1989/oy1*:B73, two with *vey1*^{Mo17}, were used for these measurements. Plants were grown in a randomized complete block design of three replicated blocks. For each genotype nine plants were measured as three replicates in each of the three blocks. The following instrument conditions were maintained throughout the measurement period: an artificial light source with an intensity of 1700 µmol photosynthetically active radiation (PAR) m^{-2} s^{-1}, air temperature of ~31 ºC, CO_2 concentration of 400 mL L^{-1}, air flow of 400 µmol s^{-1}, and relative humidity of 50-60%. Leaf temperatures varied from 32-34ºC during the measurements.

Chlorophyll fluorescence measurements were taken on the same leaves used for gas-exchange using a Handy PEA (Hansatech Instruments Ltd., Norfolk, UK). Leaves were dark-adapted for 20-30 min using leaf clips before taking measurements. The saturation pulse rate of 3000 µmol m^{-2} s^{-1} was used to measure the emission of chlorophyll fluorescence. The initial chlorophyll fluorescence yield (F_0), the variable chlorophyll fluorescence yield (F_v), and the maximum chlorophyll fluorescence yield (F_m) were recorded. The maximum photochemical efficiency of PSII in dark-adapted leaves was obtained by calculating the ratio of F_v/F_m.

Results

Negative affect of *Oy1-N1989* on flowering time is exacerbated by Mo17

While preparing the material for our previous study (Khangura *et al.* 2019), we noticed that *Oy1-N1989* exhibited a consistent delay in flowering. If this was due to variation in the accumulation of chlorophyll, or downstream consequences of changes in chlorophyll content, we expect that contribution of the *vey1* enhancing QTL from Mo17 should make this more severe. Heterozygous *Oy1-N1989* mutant plants in the Mo17 × B73 hybrid genetic background flower up to two-weeks later than wild-type siblings. The *Oy1-N1989* mutants also flower later in an isogenic inbred B73 background; however, the delay is less than half with mutants flowering four days after wild-type siblings (Figure 1; Table S4). The wild-type B73 and Mo17 F_1 hybrid plants flower earlier than the wild-type B73 inbred plants (Table S4). Maize is protandrous in nature; tassels mature earlier than the ear-inflorescence. The effect of *Oy1-N1989* and *vey1* on flowering time was similar for both anthesis and silk emergence. The window of difference in maturity of the tassel and ear inflorescence, measured as ASI, is wider in the wild-type siblings compared to the mutants in Mo17 × B73 hybrid background. However, the wild-type and mutant

siblings are not different in B73 inbred background. This is consistent with the *vey1* allele from Mo17 impacting all phenotypes recorded for *Oy1-N1989* allele to date, including delayed flowering.

Delayed flowering time of *Oy1-N1989* mutants in B73 × Mo17 mapping populations maps to *vey1*

To test whether the effect in the hybrids was the result of the *vey1* locus, or some other factor in the Mo17 background, we recording flowering time in wild-type and mutant plants of the F_1 progenies of *Oy1-N1989/oy1*:B73 pollen-parent with IBM-RILs and Syn10-DH. The crossing scheme used for line-cross experiments have been described before (Khangura *et al.* 2019). Hereafter, the hybrid populations developed from these crosses will be referred to as IBM-RILs F_1 and Syn10-DH F_1 populations (Figure 2).

Pairwise correlations were calculated between previously reported chlorophyll index measures (Khangura *et al.* 2019) and flowering time traits collected from the same plants (Tables S5 and S6). The chlorophyll index was measured at two time points CCMI (25-30 days after sowing) and CCMII (45-50 days after sowing). In both the IBM-RILs and Syn10-DH F_1 populations, significant positive correlations were observed between wild-type and mutant flowering traits. In both populations, chlorophyll measurements in the wild-type siblings (WT_CCMI and WT_CCMII) did not show any correlation with the mutant flowering time traits (Figure 3, Table S5, and S6). In the IBM-RILs crosses, wild-type CCMII displayed a weak significant negative correlation with wild-type DTA and DTS. Similarly, in the Syn10-DH crosses wild-type CCMI displayed a significant weak negative correlation with wild-type DTA and DTS. This indicates that the phenomena observed in our mutants, reduced chlorophyll content associated with a delay in flowering time, could be seen in the wild-type siblings

although the genetic basis for the variation in wild-type chlorophyll was not resolved to the *oy1* locus (Khangura *et al.* 2019). The most dramatic and obvious correlation were the negative correlation between CCM trait values (CCMI and CCMII) and flowering time in the mutant siblings in both IBM-RILs and Syn10-DH F_1 populations. The mutants in these populations also showed a clear increase in mean values for days to anthesis and silking compared to wild-type siblings (Figure 4).

The frequency distribution plot of days to anthesis in mutant siblings of IBM-RILs and Syn10-DH F_1 populations displayed a bimodal distribution, suggesting a single locus segregating in these populations as the basis of flowering time suppression of *Oy1-N1989* mutants by B73 genotype (Figure 5). QTL mapping detected a single QTL on chromosome 10 at similar linkage positions for all mutant derived flowering traits (Figure 5; Tables S7 and S8). This corresponds to the *vey1* locus that we previously described as a major QTL that controls chlorophyll pigment biosynthesis in the presence of the *Oy1-N1989* allele (Khangura *et al.* 2019). QTL mapping for number of days to flower (anthesis and silking) in the mutant heterozygotes (MT_DTA and MT_DTS), ratio of days to flower derived from mutant and wild-type siblings (Ratio_DTA and Ratio_DTS), and the difference in days to flower between the wild-type and mutant siblings (Diff_DTA and Diff_DTS) all detected *vey1* as the sole QTL in the population exceeding a permutation-estimated significance threshold (alpha<0.05) in these traits and explaining ~40-48% of the phenotypic variation in the IBM-RILs crosses, and >65% variation in the flowering traits in Syn10-DH F_1 crosses. As expected, the *Oy1-N1989* enhancing $vey1^{Mo17}$ allele was associated with a delay in flowering time in the mutant hybrid siblings (Tables S7 and S8). In addition to *vey1*, an additional QTL controlling mutant anthesis and silking was detected in the Syn10-DH F_1 population on chromosome 2 which we call *other oy1 flowering time locus1* (*oof1*). This QTL

explained ~7-8% variation with the Mo17 allele at this locus resulting in ~2-3 days of delay in reproductive maturity of mutant siblings.

Because of the very large effect of *vey1* on flowering time, and the mild segregation distortion at this locus in both bi-parental populations (Khangura *et al*. 2019), weak QTL might be detected by spurious linkage between chr2 and chr10 markers. To test this, we carried out multiple regressions using top markers at *oof1* and *vey1* as independent variables and DTA in the Syn10-DH as a dependent variable (data not shown). In this analysis, both *vey1* and *oof1* remained a significant factor in the multiple regression and explained 62% and 2% of the variance in flowering time, respectively. Inclusion of a *vey1* × *oof1* interaction term did not improve the fit of the model, did not eliminate the significance of the *oof1* term, and the interaction term was not a significant variable. Therefore, we propose that *oof1* is a novel QTL contingent upon the *Oy1-N1989* mutation and genetically independent of *vey1*.

The mechanism(s) of the flowering time delays in *Oy1-N1989* mutants does not seem similar to the effect of drought stress which differentially alters the time to silking and anthesis, commonly measured by the anthesis-silking interval (ASI). The ASI of mutant and wild-type siblings were not discernable and no QTL were detected for ASI in the mutants. In our conditions, we did not detect any QTL for flowering time in wild-type siblings (Tables S7 and S8). Thus, detection of *vey1* and *oof1* in these QTL analyses was conditioned on the presence of the *Oy1-N1989* allele suggesting a role for either photosynthesis or chlorophyll metabolites in the regulation of flowering time.

We further tested the effect of the *vey1* critical region using the BM-NIL F_1 population that has been previously described. We observed that introgression of *vey1* locus from Mo17 resulted in delaying flowering time in both B73 and Mo17 isogenic backgrounds, whereas *vey1*

introgression from B73 into Mo17 can restore the negative effect of Mo17 genotype at this position on flowering time (Figure 6, Figure S3, and Table S3). No effect of *vey1* introgression from either parent was visible on the flowering time of the wild-type siblings. Representative plants showing the delayed reproductive maturity of B73-like NILs carrying $vey1^{Mo17}$, and reciprocal introgression of $vey1^{B73}$ into Mo17 background displayed the opposite effect on flowering time (Figure 6). Thus, these results clearly show the single locus effect of *vey1* on flowering time in maize in *Oy1-N1989*-contingent manner in both isogenic inbred (B73) and hybrid (Mo17 × B73) background.

Expression polymorphism in B73-like NILs is consistent with cis-acting regulatory polymorphism at *vey1*

Our previous study looking at the suppression of *Oy1-N1989* mutant phenotype using chlorophyll accumulation identified a cis-eQTL at *oy1* in the IBM-RILs population (Khangura *et al*. 2019). Normalized expression (RPKM) of OY1 derived from 14 days old shoot apices of IBM-RILs (Li et al., 2013; 2018) were used for this analysis. The top marker, isu085b, used in the detection of this cis-eQTL was also one of the top significant markers for mutant flowering time traits (Figure S1 and Table S9). Regression of OY1 RPKM and flowering traits collected in IBM-RILs F_1 population identified a significant linear relationship between gene expression in wild-type inbred lines and flowering time measurements from mutant F_1 siblings (Figure S2 and Table S9). Roughly 21% of the variation in mutant DTA could be explained by OY1 expression in the IBM-RILs shoot apices. OY1 RPKM did not predict variation in wildtype DTA.

The allele specific-expression (ASE) assay in our previous study identified bias in expression with the wild-type *oy1* allele from Mo17 displaying relatively lower expression (Khangura *et al.* 2019). Our previous work compared mutant plants in two different genetic

backgrounds which can complicate the interpretations due to trans effect in the hybrid background. To overcome this limitation, an ASE assay was designed to test bias at *oy1* using near-isogenic lines in the B73 background. These B73-like NILs consisted of two independent NILs with *vey1*^{Mo17} introgression, and two independent NILs with B73 genotype at *vey1*. This material was grown in the field and expression of *oy1* was quantified in the top fully-expanded leaf at the V3 developmental stage. Consistent with the previous ASE results, a significantly greater proportion of expression was derived from the *Oy1-N1989* mutant allele when the wildtype *oy1* allele was contributed by *vey1*^{Mo17} introgression as compared to the isogenic mutant siblings carrying the wildtype *oy1* allele from *vey1*^{B73} locus (Table S10).

Net CO_2 assimilation and sugar metabolism is reduced in *Oy1-N1989* mutants in *vey1*-dependent manner

We measured net CO_2 assimilation, sub-stomatal CO_2, photosystem II fluorescence, and photosynthate accumulation in enhanced and suppressed *Oy1-N1989/oy1* mutants. A previous study in maize has shown that reduction in chlorophyll levels in the leaves leads to a reduction in photosynthetic rate (Huang *et al.* 2009). A similar reduction in photosynthetic rate should be displayed by *Oy1-N1989/oy1* mutants and the Mo17 allele should show a greater reduction in photosynthesis compared to the B73 allele. We tested this using F_1 progenies derived from four B73-like NILs that were crossed to *Oy1-N1989/oy1*:B73 pollen. Two of these NILs had *vey1*^{Mo17} introgression, whereas the other two had *vey1*^{B73} genotype. The negative effect of *vey1*^{Mo17} introgression on chlorophyll accumulation was visible in the *Oy1-N1989* mutant allele background (Figure 6). As expected, photosynthetic rate (A) was reduced in mutants as compared to wildtype siblings, and mutants were modified further by the *vey1* genotype (Table S11). Photosystem II efficiency (Fv/Fm) measurements indicated higher photo-oxidative damage

to the photosystem in enhanced mutant plants compared to the suppressed mutants. Wild-type siblings of all four B73-like NIL F_1 progenies showed no statistically significant difference for chlorophyll and gas-exchange measurements. This indicates that, just as for chlorophyll content, the *vey1* QTL affects net CO_2 assimilation in the presence of the *Oy1-N1989* mutant allele. No differences in stomatal conductance (g_s) or transpiration (E) was observed in the mutant plants, however, severe mutant plants showed significantly higher accumulation of intracellular CO_2 (Ci) compared to the suppressed mutants suggesting the failure of the enhanced mutant plants to uptake carbon (Table S11).

These differences in photosynthetic rate should result in a decrease of non-structural carbohydrates. The levels of non-structural carbohydrates were determined from leaves of the same mutant plants that were used for gas-exchange measurements. Levels of sucrose, glucose, fructose, and starch were measured in these samples. All of these showed a significant reduction in the enhanced mutants compared to the suppressed mutants in the B73 isogenic background (Figure 7 and Table S12). Lower levels of sugars and starch in the enhanced mutants are consistent with the observation of low photosynthetic rate in these genotypes compared to the suppressed mutant NILs.

Defoliation in *Zea mays, Sorghum bicolor,* and *Setaria viridis* delays flowering time

The existing literature suggests sugars and carbon metabolism play an important role in regulating flowering time in plants (Ohto *et al.* 2001; Seo *et al.* 2011; Wahl *et al.* 2013). We hypothesized that removal of source tissue should mimic sugar starvation observed in *Oy1-N1989* mutants. As a result, defoliation should result in delayed flowering in defoliated (treated) plants compared to non-defoliated (control) plants. We tested this hypothesis using the wild-type inbred strains in maize and two other monocot species: *Sorghum bicolor* (sorghum) and *Setaria*

viridis (green foxtail). Each species was defoliated at an early vegetative stage when only a few leaves had fully expanded. The intent was to deprive plants of leaf area and photosynthate early in development to separate the loss of chlorophyll and the loss of photosynthate, which are coupled in the *Oy1-N1989* mutant study. Defoliation delayed flowering in all the plant species tested (Figure 8). Maize, sorghum, and green foxtail displayed a delay in flowering by about 13, 7, and 4 days, respectively, compared to the control plants. Therefore, based on the defoliation study in multiple monocot species we propose that early season defoliation results in the removal of source tissue that might be critical for vegetative to floral transition in plants. Surprisingly, one-week post-defoliation, newly emerged leaves displayed a pale leaf color. Chlorophyll estimation using CCM found a reduction in the leaf greenness in the defoliated treatments compared to the control samples (Figure 8). Maize, sorghum, and green foxtail showed ~35%, ~48%, and ~58% reduction in chlorophyll, respectively, in the newly emerging leaves in the treated plants compared to the control plants. Subsequent leaves emerging from the defoliated treatments displayed normal leaf color suggesting recovery of the plants from defoliation stress. Thus, the delay in flowering time is likely due to a loss of resources (carbon reserves) but cannot be formally distinguished from a change in chlorophyll accumulation.

Leaf senescence is suppressed by *Oy1-N1989* mutants in a *vey1*-dependent manner

Leaf senescence can be induced in maize by sucrose accumulation in the leaves. This can be accomplished genetically by disrupting sucrose transport (Braun *et al.* 2006; Baker and Braun 2008; Slewinski *et al.* 2009) or by preventing the maize ears from acting as a sink (Allison and Weinmann 1970; Sekhon *et al.* 2012, 2019). In maize, previous studies have shown that leaf senescence caused by pollination prevention or ear removal before pollination is genotype-dependent (Ceppi et al. 1987; Allison and Weinmann 1970). We found that levels of free sugars

and starch were significantly lower in the young leaves of enhanced *Oy1-N1989* mutant B73 NILs compared to the suppressed mutant NILs (Figure 8). If the accumulation of sugars in the leaves is a pre-requisite for leaf senescence, we expected delayed senescence in the *Oy1-N1989* mutants and for this to vary in a *vey1* dependent manner. We tested the effect of this differential sugar accumulation in mutant B73-like NILs on induced leaf senescence by pollination avoidance. We observed that 30 days-after-anthesis (DAA), the top leaves of the unpollinated wild-type B73 plants showed complete senescence of the leaves with only a few green patches. Unpollinated *Oy1-N1989* mutant plants in the suppressed B73 NIL background did not show such an extreme phenotype but rather, showed only a few patches of anthocyanin accumulation and cell death by 30 DAA (Figure 9). On the other hand, unpollinated mutant plants in B73 NIL background with $vey1^{Mo17}$ introgression did not show any sign of leaf senescence at 30 DAA. At 42 DAA, unpollinated wild-type and mutants with and without $vey1^{Mo17}$ genotype showed leaf senescence, however, the enhancement of *Oy1-N1989* by the $vey1^{Mo17}$ resulted in substantially less cell death and anthocyanin accumulation.

Discussion

Our previous work identified a modifier, *vey1*, that affects the chlorophyll accumulation in *Oy1-N1989/oy1* heterozygotes (Khangura *et al.* 2019). The *vey1* polymorphism(s) are common natural variant(s) linked to the *oy1* locus of maize. We proposed that *vey1* results from cis-acting regulatory polymorphisms that affect the expression of OY1. The suppression of the mutant, and accumulation of chlorophyll, follows the proportion of wild-type and mutant transcript levels (Table S10 and Khangura *et al.* 2019). In this work, we describe a delay in flowering in the *Oy1-N1989* mutants and demonstrate that *vey1* encodes a strong modifying QTL altering the

flowering time of mutant siblings in all mapping populations (Figures 5 and 6; Tables S7 and S8). Just as the detection of *vey1* for CCM was contingent on *Oy1-N1989* mutant allele in the background, there was no effect of *vey1* on flowering time in wild-type siblings. We observed the same marker, isu085b, had the strongest effect on chlorophyll content, OY1 transcript abundance in shoot apices (Khangura *et al.* 2019) and variation in flowering time of IBM-RILs x *Oy1-N1989* mutant F_1 mutant siblings (Table S9 and Figure S2). Taking these observations together, we propose that the cis-acting eQTL at *oy1* is affecting chlorophyll level in *Oy1-N1989* mutants, and that the alteration in photosynthesis through perturbed chlorophyll metabolism affects flowering time variation in mutant siblings in these populations.

Our previous work on *vey1* has focused on the cryptic nature of the variation, and the interaction between the *vey1* QTL and the *Oy1-N1989* mutant allele. However, the experiments presented here clearly transcend this limitation and identify chlorophyll content as a heretofore unappreciated correlate, if not determinant, of flowering time affecting even in wild-type siblings (Figure 3; Tables S5 and S6). We observed that CCM values, especially CCMII in IBM-RILs and CCMI in Syn10-DH F_1 populations, were negatively correlated with wild-type flowering time measurements. This suggests a role for the normal variation in chlorophyll contents in the control of flowering time in maize either via changes to photosynthetic output or signaling. As no QTL were detected for CCM in the wild-type siblings in our previous work (Khangura *et al.* 2019), it also suggests that mechanism responsible for CCM and flowering time covariation is likely independent of *vey1*. This is further strengthened by the absence of an effect of *vey1* on flowering time in the wild-type siblings in our NILs (Table S3 and Figure S3). It is possible that flowering time QTL segregating in the B73 × Mo17 cross are fortuitously linked to other loci affecting CCM in wild-type plants, which did not pass the threshold of detection in our QTL

experiments. Otherwise there should be no formal relationship between CCM and flowering time in other populations with greater recombination or different alleles, such as in an association panel. Further experiments are required to validate or reject the causal nature of the relationships between CCM and flowering time in wild-type siblings of this material.

Even though Syn10-DH and IBM-RILs are derived from the same parents, they differ in the method of development and rates of recombination (Liu et al. 2015; Hussain et al. 2007; Lee et al. 2002). Thus, these two populations yield different levels of resolution for QTL detection. Our previous analysis to fine map *vey1* QTL using CCM values showed Syn10-DH to have a higher mapping resolution than the IBM-RILs population (Khangura *et al.* 2019). We also observed different QTL for flowering time in these populations. QTL analysis in Syn10-DH F_1 population detected the *oof1* QTL on chromosome 2 affecting MT_DTA and MT_DTS as well as the major-effect locus *vey1* (Table S8). The detection of *oof1* was dependent on the presence of the *Oy1-N1989* mutant, but was neither contingent on nor displayed any epistatic interactions with *vey1* as assessed by multiple regression. Thus, *oof1* appears to be a novel locus of independent mechanism affecting flowering time in the *Oy1-N1989* mutants. This QTL on chromosome 2 was not detected for any other trait in the Syn10-DH and IBM-RILs testcross populations with *Oy1-N1989/oy1*:B73 in the current study nor was it identified as a modifier of chlorophyll content in our previous study (Khangura *et al.* 2019). The amount of phenotypic variation explained by *vey1* in flowering time was higher in Syn10-DH experimental material than the IBM-RILs testcross population by ~20% (Tables S7 and S8). Greater variation in flowering time in the IBM-RILs testcross progenies that could not be modeled by marker genotypes may result from higher residual heterozygosity or greater rates of pollen contamination during the single seed descent (SSD) procedure used to generate the IBM-RILs

(Lee et al. 2002). Heterozygosity is expected to be negligible in Syn10-DH population because of the DH procedure employed to fix allele segregation during population development (Hussain *et al.* 2007). In addition, we had a moderate increase in sample size in the Syn10-DH (251 lines) as compared to the IBM-RILs (216 lines) that is expected to result in a marginally greater power to detect QTL in the Syn10-DH F_1 populations.

Chlorophyll levels are correlated with the rate of photosynthesis in plants (Huang *et al.* 2009). Some controversy has been reported in mutants of soybean affected in an ortholog of *oy1* with some reports showing little impact on photosynthesis (Sakowska *et al.* 2018)and others clearly demonstrating a linear relationship between chlorophyll variation and photosynthesis (Walker *et al.* 2017). The reasons for conflicting conclusions results from soybean mutants are not fully clear but it warrants some caution in making simplistic interpretations about the impact of chlorophyll deficient mutants on photosynthesis. In our study, net CO_2 assimilation was associated with the severity of the *Oy1-N1989* mutant phenotype. The effect of chlorophyll loss on CO_2 assimilation measurements using a LICOR instrument was somewhat non-linear. A nearly 5-fold reduction in CCM in *Oy1-N1989* NILs carrying a B73 allele at *vey1* resulted in in a 22% reduction in net CO_2 assimilation while the 10-fold reduction in CCM in *Oy1-N1989* NILs carrying a Mo17 allele at *vey1* resulted in a 64% reduction in net photosynthetic rate, compared to their isogenic wildtype siblings (Table S11). Ultimately, both reductions resulted in less accumulation of free sugars and starch, with a substantially greater reduction in the enhanced mutant NILs (Figure 7; Tables S11 and S12). The allelic interactions of *Oy1-N1989* and wild-type *oy1* alleles are consistent with the inductive role of carbon status on floral transition (Ohto et al. 2001; Seo et al. 2011; Wahl et al. 2013; Minow et al. 2018). Additional work exploring proposed carbon signaling metabolites, such as T6P and organic acids, and analyses of the

downstream floral integrators such as the FT orthologs of maize are still needed to link our results to the existing models of floral transition regulation in maize (Minow *et al.* 2018). One complexity that we observed in our data is that the alternate experiments such as defoliation were not able to distinguish photosynthate levels from changes in chlorophyll (Figure 8). The mechanical removal of leaves resulted in changes to CCM. Two other subunits of magnesium chelatase are encoded by genes that were identified in Arabidopsis as *genomes uncoupled* mutants, *gun4* and *gun5*, with altered retrograde, plastid-to-nuclear, signaling with defects in chlorophyll metabolism (Susek *et al.* 1993; Mochizuki *et al.* 2001; Larkin *et al.* 2003). Multiple studies have demonstrated retrograde signaling mutants with defects in chlorophyll metabolism (Hernández-Verdeja and Strand 2018) and circadian rhythm (Jones 2019). Retrograde signaling events are also associated with cell death, chloroplast development, and etiolation but it acts via a number of modifiers of flowering, including phytochromes, phytochrome signaling components, blue light perception via *crytochrome1*, and circadian rhythmicity of key genes that affect flowering time. Additional experiments are necessary to clearly separate the effects of chlorophyll metabolite levels from photosynthate levels to independently test their effects on flowering time.

We have known that defoliation is practiced in some maize nurseries to stagger flowering time and permit intercrossing of lines with divergent reproductive maturities. We had presumed that this was based on published research. Remarkably, we were not able to find a reference for this practice. Previous work on defoliation in maize has looked at the effect of early and late season defoliation on growth, and yield components but did not report flowering times (Crookston and Hicks 1988; Pearson and Fletcher 2009). As a result, Figure 8 provides information we already knew as a research community and have been sharing informally but

have not described formally. In addition, we extended this observation from maize to both sorghum and green foxtail, indicating that defoliation can achieve staggered flowering times in these species as well. This may be a general feature of grasses, but appears to not be universal in angiosperms as early-season defoliation of photoperiod-sensitive strawberries did not affect flowering time (Guttridge 1959). Surprisingly, the defoliation of maize, sorghum, and green foxtail resulted in reduced chlorophyll in the new leaves. As a result, a mechanical treatment that was expected to only affect photosynthetic leaf area, and not chlorophyll content, served to highlight the interconnected nature of plant metabolism: large changes to any feature of central metabolism or plant physiology result in large changes to all of central metabolism and plant physiology. Carefully conceived narrow manipulation of the metabolites and additional studies of mechanisms of flowering time modulation are required to determine how chlorophyll metabolism influences flowering time.

Sugar export mutants in maize that carry lesions in *sut1*, *tdy1*, *tdy2*, *psc*, or *sxd1* have all been shown to delay flowering time (Braun *et al.* 2006; Baker and Braun 2008; Ma *et al.* 2008; Slewinski *et al.* 2009; Slewinski and Braun 2010). We also observed declines in sugar levels in *Oy1-N1989* mutants (Figure 7 and Table S12) and a delay in flowering time (Figure 1). It is tempting to consider these mutants as a demonstration that sugar signaling can work independent of chlorophyll, but these mutants also display low chlorophyll contents (Braun *et al.* 2006; Baker and Braun 2008; Ma *et al.* 2008; Slewinski *et al.* 2009; Slewinski and Braun 2010). Curiously, *sxd1* encodes tocopherol cyclase (Porfirova *et al.* 2002; Sattler *et al.* 2003). Tocopherol and chlorophyll share the phytol side chain, and the salvage pathway for phytol side chains from chlorophyll can contribute to tocopherol accumulation in both maize and Arabidopsis (Ischebeck *et al.* 2006; Schelbert *et al.* 2009; Diepenbrock *et al.* 2017). While it is attractive to try and unify

these findings, chlorophyll breakdown products were only rate limiting for tocopherol synthesis in senescent tissues of Arabidopsis (Zhang *et al*. 2014). Furthermore, in *Oy1-N1989* mutants the phytol precursors should be abundant as this pool is not being consumed by chlorophyll biosynthesis. Future experiments that more carefully explore these metabolites, for instance, via other mutants that do not simultaneously affect multiple pathways are required. The finding that defoliation impacts flowering time and the same biochemical and molecular responses as observed in the photosynthetically compromised *Oy1-N1989* mutants may also provide mechanistic insights for this phenomenon.

Accumulation of sugars in the leaves due to sink disruption has been proposed to induce leaf senescence in a variety of angiosperms, including maize and Arabidopsis (Allison and Weinmann 1970; Ceppi *et al*. 1987; Pourtau *et al*. 2006; Sekhon *et al.* 2012, 2019). In maize, leaf senescence is triggered when pollination is prevented and sucrose accumulates in leaves due to the lack of the sink activity of a pollinated ear (Ceppi et al. 1987; Allison and Weinmann 1970). This sucrose-dependent leaf senescence is genotype-dependent, and B73 is particularly susceptible to this phenomenon. Genetic inheritance of the induced senescence phenomenon in maize inbred line B73 is proposed to be under the control of a single dominant locus (Ceppi *et al.* 1987). The leaf senescent phenotypes of the sucrose export mutants demonstrate that excessive photosynthate accumulation can cause tissue to senesce regardless of ear presence (Braun *et al.* 2006; Baker and Braun 2008; Ma *et al*. 2008; Slewinski *et al.* 2009). Induced leaf senescence by sink removal or sugar application shows some overlap of biochemical and molecular mechanisms with natural senescence in plants (summarized in Sekhon et al. 2012). A study of gene expression in the B73 inbred of maize identified Senescence Associated Genes (SAGs) that exhibit gene expression changes during pollination-prevented leaf senescence (Sekhon et al.

2012). We found that leaf senescence could be prevented or delayed by the suppression of photosynthesis in the *Oy1-N1989* mutant and further modulated by *vey1* variants. We expect that future gene expression studies in *Oy1-N1989* mutants and carbon export mutants will identify genes consistently impacted by lower and higher chlorophyll levels, presumably including SAGs and genes regulating carbon metabolism.

Conclusions

Flowering time in plants is regulated by environmental and endogenous cues. In this study, we demonstrate that the interaction between natural and induced variation at the *oy1* locus of maize, encoding the magnesium chelatase subunit I responsible for the first committed step of chlorophyll biosynthesis, regulates flowering time. The effect of *oy1* variation on flowering time and other physiological traits is consistent with the previously proposed and widely-accepted role of photosynthetically derived sugars on flowering time. The previously identified *vey1* QTL, a putative cis-acting polymorphism(s) in the regulatory region proximal to *oy1*, modified the flowering time delay in the *Oy1-N1989* mutant heterozygotes. Further, *vey1* and *Oy1-N1989* affected gas-exchange parameters, chlorophyll fluorescence, sugar accumulation, and starch accumulation in the immature leaves of *Oy1-N1989* mutant plants. Thus, all data are consistent with *Oy1-N1989* altering flowering time by perturbing carbon fixation via photosynthesis.

Acknowledgements

R.S.K. was supported by USAID Feed the Future CGIAR-US Initiative grant “Heat stress resilient maize for South Asia through a public-private partnership” awarded to G.S.J. We would also like to thank financial support by NSF grant 1444503 awarded to G.S.J. and B.P.D. We

thank the Purdue ACRE and ICSC staff members Mr. Jim Beaty and Mr. Jason Adams for help with planting, and management of the field experiments described in this work. We also thank past Johal lab members for help with planting and data collection. We would like to thank Mike Gosney for helping with gas-exchange measurements. We gratefully acknowledge the bobcat operator for dumping loads of gravel on our office walls while we attempted to write this paper. Solidarity with all.

REFERENCES

Abe, M., Y. Kobayashi, S. Yamamoto, Y. Daimon, A. Yamaguchi *et al.*, 2005 FD , a bZIP Protein Mediating Signals from the Floral Pathway Integrator FT at the Shoot Apex. Science 309: 1052–1056.

Allison, J. C. S., and H. Weinmann, 1970 Effect of Absence of Developing Grain on and Senescence of Maize Leaves. Plant Physiol. 46: 435–436.

Alter, P., S. Bircheneder, L.-Z. Zhou, U. Schlüter, M. Gahrtz *et al.*, 2016 Flowering Time-Regulated Genes in Maize Include the Transcription Factor ZmMADS1. Plant Physiol. 172: 389–404.

Amasino, R. M., and S. D. Michaels, 2010 The Timing of Flowering. Plant Physiol. 154: 516–520.

Baker, R. F., and D. M. Braun, 2008 Tie-dyed2 functions with tie-dyed1 to promote carbohydrate export from maize leaves. Plant Physiol. 146: 1085–1097.

Bomblies, K., R.-L. Wang, B. A. Ambrose, R. J. Schmidt, R. B. Meeley *et al.*, 2003 Duplicate FLORICAULA/LEAFY homologs zfl1 and zfl2 control inflorescence architecture and flower patterning in maize. Development 130: 2385–2395.

Bouchet, S., P. Bertin, T. Presterl, P. Jamin, D. Coubriche *et al.*, 2017 Association mapping for phenology and plant architecture in maize shows higher power for developmental traits compared with growth influenced traits. Heredity (Edinb). 118: 249–259.

Braun, D. M., Y. Ma, N. Inada, M. G. Muszynski, and R. F. Baker, 2006 tie-dyed1 Regulates carbohydrate accumulation in maize leaves. Plant Physiol. 142: 1511–22.

Broman, K. W., H. Wu, S. Sen, and G. a. Churchill, 2003 R/qtl: QTL mapping in experimental crosses. Bioinformatics 19: 889–890.

Buckler, E. S., J. B. Holland, P. J. Bradbury, C. B. Acharya, P. J. Brown *et al.*, 2009 The genetic architecture of maize flowering time. Science 325: 714–718.

Ceppi, D., M. Sala, E. Gentinetta, A. Verderio, and M. Motto, 1987 Genotype-Dependent Leaf Senescence in Maize INHERITANCE AND EFFECTS OF POLLINATION-PREVENTION. Plant Physiol. 85: 720–725.

Chen, M., J. Chory, and C. Fankhauser, 2004 Light Signal Transduction in Higher Plants. Annu. Rev. Genet. 38: 87–117.

Cho, L. H., R. Pasriga, J. Yoon, J. S. Jeon, and G. An, 2018 Roles of Sugars in Controlling Flowering Time. J. Plant Biol. 61: 121–130.

Cho, L. H., J. Yoon, and G. An, 2017 The control of flowering time by environmental factors. Plant J. 90: 708–719.

Colasanti, J., Z. Yuan, and V. Sundaresan, 1998 The indeterminate gene encodes a zinc finger protein and regulates a leaf-generated signal required for thetransition to flowering in maize. Cell 93: 593–603.

Coles, N. D., M. D. McMullen, P. J. Balint-Kurti, R. C. Pratt, and J. B. Holland, 2010 Genetic control of photoperiod sensitivity in maize revealed by joint multiple population analysis. Genetics 184: 799–812.

Coneva, V., D. Guevara, S. J. Rothstein, and J. Colasanti, 2012 Transcript and metabolite signature of maize source leaves suggests a link between transitory starch to sucrose balance and the autonomous floral transition. J. Exp. Bot. 63: 5079–5092.

Coneva, V., T. Zhu, and J. Colasanti, 2007 Expression differences between normal and indeterminate1 maize suggest downstream targets of ID1, a floral transition regulator in maize. J. Exp. Bot. 58: 3679–3693.

Corbesier, L., P. Lejeune, and G. Bernier, 1998 The role of carbohydrates in the induction of flowering in Arabidopsis thaliana: Comparison between the wild type and a starchless mutant. Planta 206: 131–137.

Corbesier, L., C. Vincent, S. Jang, F. Fornara, Q. Fan *et al.*, 2007 FT protein movement contributes to long-distance signaling in floral induction of Arabidopsis. Science 316: 1030–1033.

Crookston, R. K., and D. R. Hicks, 1988 Effect of Early Defoliation on Maize Growth and Yield: an Eleven-year Perspective. Crop Sci. 28: 371–373.

Danilevskaya, O. N., X. Meng, D. A. Selinger, S. Deschamps, P. Hermon *et al.*, 2008 Involvement of the MADS-Box Gene ZMM4 in Floral Induction and Inflorescence Development in Maize. Plant Physiol. 147: 2054–2069.

DePristo, M. A., E. Banks, R. Poplin, K. V Garimella, J. R. Maguire *et al.*, 2011 A framework for variation discovery and genotyping using next-generation DNA sequencing data. Nat. Genet. 43: 491–498.

Diepenbrock, C. H., C. B. Kandianis, A. E. Lipka, M. Magallanes-Lundback, B. Vaillancourt *et al.*, 2017 Novel Loci Underlie Natural Variation in Vitamin E Levels in Maize Grain. Plant Cell 29: 2374–2392.

Doebley, J., A. Stec, and L. Hubbard, 1997 The evolution of apical dominance in maize. Nature 386: 485–488.

Eichten, S. R., J. M. Foerster, N. de Leon, Y. Kai, C.-T. Yeh *et al.*, 2011 B73-Mo17 near-isogenic lines demonstrate dispersed structural variation in maize. Plant Physiol. 156: 1679–90.

Evans, M. M., and R. S. Poethig, 1995 Gibberellins promote vegetative phase change and reproductive maturity in maize. Plant Physiol. 108: 475–87.

Eveland, A. L., and D. P. Jackson, 2012 Sugars, signalling, and plant development. J. Exp. Bot. 63: 3367–3377.

Gibson, L. C. D., R. D. Willows, C. G. Kannangara, D. von Wettstein, and C. N. Hunter, 1995 Magnesium-protoporphyrin chelatase of Rhodobacter sphaeroides: reconstitution of activity by combining the products of the bchH, -I, and -D genes expressed in Escherichia coli. Proc. Natl. Acad. Sci. U. S. A. 92: 1941–1944.

Guttridge, C. G., 1959 Evidence for a Flower Inhibitor and Vegetative Growth Promoter in the

Strawberry. Ann. Bot. 23: 351–360.

Hernández-Verdeja, T., and Å. Strand, 2018 Retrograde Signals Navigate the Path to Chloroplast Development. Plant Physiol. 176: 967–976.

Huang, M., T. L. Slewinski, R. F. Baker, D. Janick-Buckner, B. Buckner *et al.*, 2009 Camouflage patterning in maize leaves results from a defect in porphobilinogen deaminase. Mol. Plant 2: 773–89.

Huang, C., H. Sun, D. Xu, Q. Chen, Y. Liang *et al.*, 2017 ZmCCT9 enhances maize adaptation to higher latitudes. Proc. Natl. Acad. Sci. 115: E334–E341.

Hung, H.-Y., L. M. Shannon, F. Tian, P. J. Bradbury, C. Chen *et al.*, 2012 ZmCCT and the genetic basis of day-length adaptation underlying the postdomestication spread of maize. Proc. Natl. Acad. Sci. 109: E1913–E1921.

Hussain, T., P. Tausend, G. Graham, and J. Ho, 2007 Registration of IBM2 SYN10 Doubled Haploid Mapping Population of Maize. J. Plant Regist. 1: 81.

Ischebeck, T., A. M. Zbierzak, M. Kanwischer, and P. Dörmann, 2006 A salvage pathway for phytol metabolism in Arabidopsis. J. Biol. Chem. 281: 2470–2477.

Jones, M. A., 2019 Retrograde signalling as an informant of circadian timing. New Phytol. 221: 1749–1753.

Karl, J., 2016 Maize Leafy1 45ft. Maize Genet. Coop. Newsl. 90: 1–15.

Khangura, R. S., S. Marla, B. P. Venkata, N. J. Heller, G. S. Johal *et al.*, 2019 A Very Oil Yellow1 Modifier of the Oil Yellow1-N1989 Allele Uncovers a Cryptic Phenotypic Impact of Cis-regulatory Variation in Maize. G3 9: 375–390.

Kozaki, A., S. Hake, and J. Colasanti, 2004 The maize ID1 flowering time regulator is a zinc finger protein with novel DNA binding properties. Nucleic Acids Res. 32: 1710–1720.

Lang, A., 1952 Physiology of Flowering. Ann. Rev. Plant. Physiol. 3: 265–306.

Lang, A., 1957 The effect of gibberellin upon flower formation. Proc. Natl. Acad. Sci. 43: 709–717.

Larkin, R. M., J. M. Alonso, J. R. Ecker, and J. Chory, 2003 GUN4, a regulator of chlorophyll synthesis and intracellular signaling. Science 299: 902–906.

Leach, K. A., and D. M. Braun, 2016 Soluble Sugar and Starch Extraction and Quantification from Maize (*Zea mays*) Leaves. Curr. Protoc. Plant Biol. 1: 139–161.

Leach, K. A., T. M. Tran, T. L. Slewinski, R. B. Meeley, and D. M. Braun, 2017 Sucrose transporter2 contributes to maize growth, development, and crop yield. J. Integr. Plant Biol. 59: 390–408.

Lee, M., N. Sharopova, W. D. Beavis, D. Grant, M. Katt *et al.*, 2002 Expanding the genetic map of maize with the intermated B73 x Mo17 (IBM) population. Plant Mol. Biol. 48: 453–61.

Liang, Y., Q. Liu, X. Wang, C. Huang, G. Xu *et al.*, 2019 ZmMADS69 functions as a flowering activator through the ZmRap2.7-ZCN8 regulatory module and contributes to maize flowering time adaptation. New Phytol. 221: 2335–2347.

Liu, H., Y. Niu, P. J. Gonzalez-Portilla, H. Zhou, L. Wang *et al.*, 2015 An ultra-high-density

map as a community resource for discerning the genetic basis of quantitative traits in maize. BMC Genomics 16: 1078.

Ma, Y., R. F. Baker, M. Magallanes-Lundback, D. Dellapenna, and D. M. Braun, 2008 Tie-dyed1 and Sucrose export defective1 act independently to promote carbohydrate export from maize leaves. Planta 227: 527–538.

Meng, X., M. G. Muszynski, and O. N. Danilevskaya, 2011 The FT-Like ZCN8 Gene Functions as a Floral Activator and Is Involved in Photoperiod Sensitivity in Maize. Plant Cell 23: 942–960.

Minow, M. A. A., L. M. Ávila, K. Turner, E. Ponzoni, I. Mascheretti *et al.*, 2018 Distinct gene networks modulate floral induction of autonomous maize and photoperiod-dependent teosinte. J. Exp. Bot. 69: 2937–2952.

Mochizuki, N., J. a Brusslan, R. Larkin, a Nagatani, and J. Chory, 2001 Arabidopsis genomes uncoupled 5 (GUN5) mutant reveals the involvement of Mg-chelatase H subunit in plastid-to-nucleus signal transduction. Proc. Natl. Acad. Sci. U. S. A. 98: 2053–2058.

Moghaddam, M. R. B., and W. Van den Ende, 2013 Sugars, the clock and transition to flowering. Front. Plant Sci. 4: 1–6.

Muszynski, M. G., T. Dam, B. Li, D. M. Shirbroun, Z. Hou *et al.*, 2006 delayed flowering1 Encodes a basic leucine zipper protein that mediates floral inductive signals at the shoot apex in maize. Plant Physiol. 142: 1523–1536.

Mutasa-Göttgens, E., and P. Hedden, 2009 Gibberellin as a factor in floral regulatory networks. J. Exp. Bot. 60: 1979–1989.

Ohto, M.-A., K. Onai, Y. Furukawa, E. Aoki, T. Araki *et al.*, 2001 Effects of Sugar on Vegetative Development and Floral Transition in Arabidopsis. Plant Physiol. 127: 252–261.

Paul, M. J., 2008 Trehalose 6-phosphate: a signal of sucrose status. Biochem. J. 412: 1–2.

Pearson, A., and A. L. Fletcher, 2009 Effect of total defoliation on maize growth and yield. Agron. New Zeal. 39: 1–6.

Porfirova, S., E. Bergmuller, S. Tropf, R. Lemke, and P. Dormann, 2002 Isolation of an Arabidopsis mutant lacking vitamin E and identification of a cyclase essential for all tocopherol biosynthesis. Proc. Natl. Acad. Sci. 99: 12495–12500.

Pourtau, N., R. Jennings, E. Pelzer, J. Pallas, and A. Wingler, 2006 Effect of sugar-induced senescence on gene expression and implications for the regulation of senescence in Arabidopsis. Planta 224: 556–568.

R core Team, 2013 R: A language and environment for statistical computing. R Foundation for Statistical Computing, Vienna, Austria. ISBN 3-900051-07-0, http://www.R-project.org/.

Sakowska, K., G. Alberti, L. Genesio, A. Peressotti, G. Delle Vedove *et al.*, 2018 Leaf and canopy photosynthesis of a chlorophyll deficient soybean mutant. Plant Cell Environ. 41: 1427–1437.

Salvi, S., G. Sponza, M. Morgante, D. Tomes, X. Niu *et al.*, 2007 Conserved noncoding genomic sequences associated with a flowering-time quantitative trait locus in maize. Proc. Natl. Acad. Sci. U. S. A. 104: 11376–11381.

Samach, A., H. Onouchi, S. E. Gold, G. S. Ditta, Z. Schwarz- *et al.*, 2000 Distinct Roles of CONSTANS Target Genes in Reproductive Development of Arabidopsis. Science 288: 1613–1616.

Sattler, S. E., E. B. Cahoon, S. J. Coughlan, and D. Dellapenna, 2003 Characterization of Tocopherol Cyclases from Higher Plants and Cyanobacteria . Evolutionary Implications for Tocopherol Synthesis and Function. Plant Physiol. 132: 2184–2195.

Sawers, R. J. H., J. Viney, P. R. Farmer, R. R. Bussey, G. Olsefski *et al.*, 2006 The maize Oil yellow1 (Oy1) gene encodes the I subunit of magnesium chelatase. Plant Mol. Biol. 60: 95–106.

Schelbert, S., S. Aubry, B. Burla, B. Agne, F. Kessler *et al.*, 2009 Pheophytin Pheophorbide Hydrolase (Pheophytinase) Is Involved in Chlorophyll Breakdown during Leaf Senescence in Arabidopsis. Plant Cell 21: 767–785.

Searle, N. E., 1965 Physiology of Flowering. Ann. Rev. Plant. Physiol. 16: 97–118.

Sekhon, R. S., K. L. Childs, N. Santoro, C. E. Foster, C. R. Buell *et al.*, 2012 Transcriptional and Metabolic Analysis of Senescence Induced by Preventing Pollination in Maize. Plant Physiol. 159: 1730–1744.

Sekhon, R. S., C. Saski, R. Kumar, B. Flinn, F. Luo *et al.*, 2019 Integrated Genome-Scale Analysis Identifies Novel Genes and Networks Underlying Senescence in Maize. Plant Cell tpc.00930.2018.

Sen, T. Z., L. C. Harper, M. L. Schaeffer, C. M. Andorf, T. E. Seigfried *et al.*, 2010 Choosing a genome browser for a Model Organism Database: surveying the Maize community. Database 2010: 1–9.

Seo, P. J., J. Ryu, S. K. Kang, and C. M. Park, 2011 Modulation of sugar metabolism by an INDETERMINATE DOMAIN transcription factor contributes to photoperiodic flowering in Arabidopsis. Plant J. 65: 418–429.

Slewinski, T. L., and D. M. Braun, 2010 The Psychedelic genes of maize redundantly promote carbohydrate export from leaves. Genetics 185: 221–232.

Slewinski, T. L., A. Garg, G. S. Johal, and D. M. Braun, 2010 Maize SUT1 functions in phloem loading. Plant Signal. Behav. 5: 1–4.

Slewinski, T. L., R. Meeley, and D. M. Braun, 2009 Sucrose transporter1 functions in phloem loading in maize leaves. J. Exp. Bot. 60: 881–892.

Steinhoff, J., W. Liu, J. C. Reif, G. Della Porta, N. Ranc *et al.*, 2012 Detection of QTL for flowering time in multiple families of elite maize. Theor. Appl. Genet. 125:.

Susek, R. E., F. M. Ausubel, and J. Chory, 1993 Signal Transduction Mutants of Arabidopsis Uncouple Nuclear CAB and RBCS Gene Expression from Chloroplast Development. Cell 74: 787–799.

Swarts, K., R. M. Gutaker, B. Benz, M. Blake, R. Bukowski *et al.*, 2017 Genomic estimation of complex traits reveals ancient maize adaptation to temperate North America. Science 357: 512–515.

Vega, S. H., M. Sauer, J. A. J. Orkwiszewski, and S. Poethig, 2002 The early phase change gene

in Maize. Plant Cell 14: 133–147.

Wahl, V., J. Ponnu, A. Schlereth, S. Arrivault, T. Langenecker *et al.*, 2013 Regulation of flowering by Trehalose-6-phosphate signalling in Arabidopsis thaliana. Science 339: 704–708.

Walker, B. J., D. T. Drewry, R. A. Slattery, A. VanLoocke, Y. B. Cho *et al.*, 2017 Chlorophyll can be reduced in crop canopies with little penalty to photosynthesis. Plant Physiol. 176: 1215–1232.

Walker, C. J., and J. D. Weinstein, 1991 In vitro assay of the chlorophyll biosynthetic enzyme Mg-chelatase: resolution of the activity into soluble and membrane-bound fractions. Proc. Natl. Acad. Sci. U. S. A. 88: 5789–5793.

Wang, R. L., A. Stec, J. Hey, L. Lukens, and J. Doebley, 1999 The limits of selection during maize domestication. Nature 398: 236–239.

Wigge, P. A., M. C. Kim, K. E. Jaeger, W. Busch, M. Schmid *et al.*, 2005 Integration of Spatial and Temporal Information During Floral Induction in Arabidopsis. Science 309: 1056–1059.

Zeevaart, J. A. D., 1962 Physiology of Flowering. Science 137: 723–731.

Zhang, W., T. Liu, G. Ren, S. Hörtensteiner, Y. Zhou *et al.*, 2014 Chlorophyll Degradation: The Tocopherol Biosynthesis-Related Phytol Hydrolase in Arabidopsis Seeds Is Still Missing. Plant Physiol. 166: 70–79.

Zhang, L., H. Yu, S. Lin, and Y. Gao, 2016 Molecular Characterization of FT and FD Homologs from Eriobotrya deflexa Nakai forma koshunensis. Front. Plant Sci. 7: 1–10.

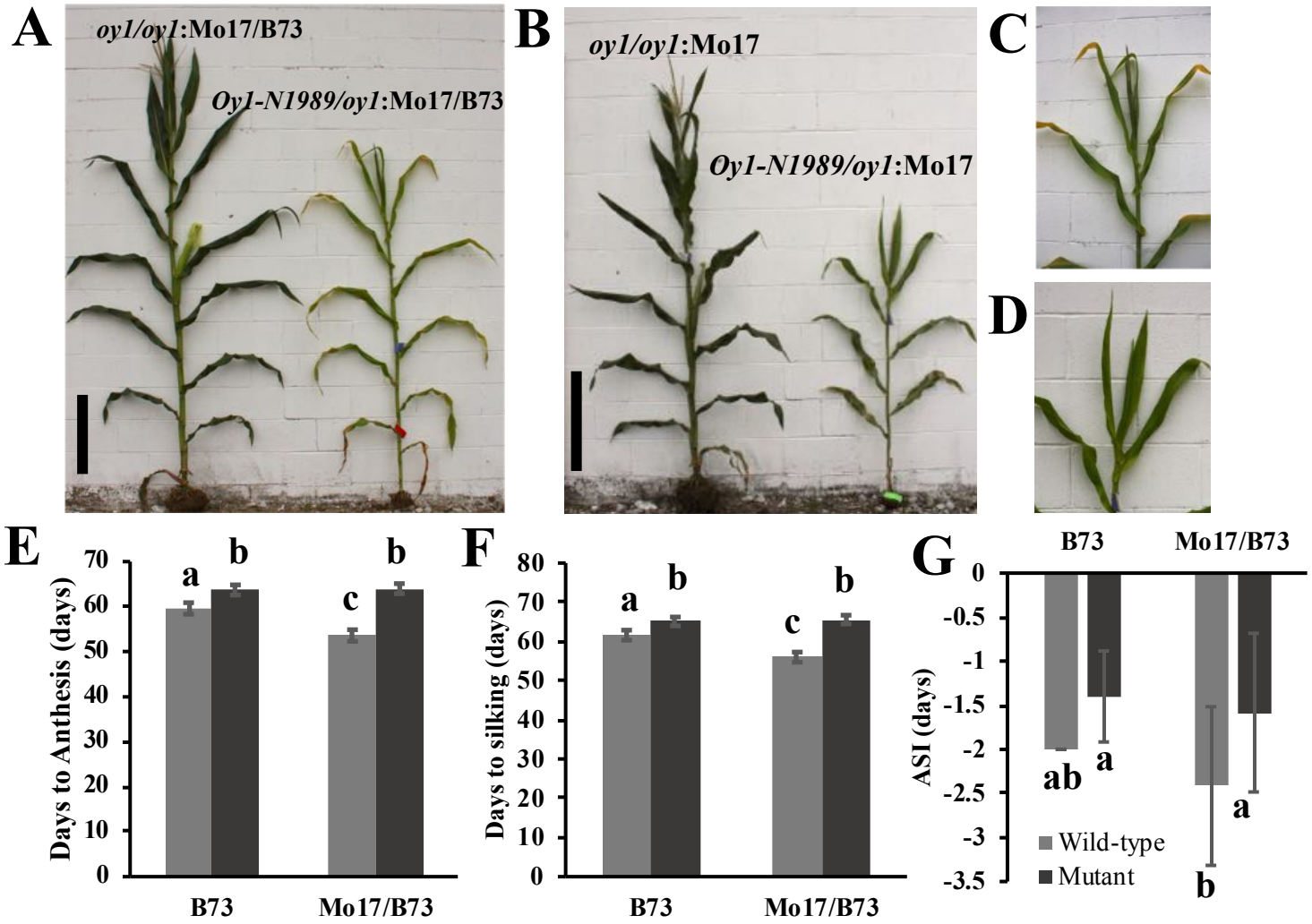

Figure 1. Reproductive maturity is delayed by *Oy1-N1989* allele in maize (A) Wild-type (left) and mutant (right) sibling from Mo17 x *Oy1-N1989/oy1*:B73 cross (reproduced from Figure 1b from Khangura *et. al*., 2019), black scale bar = 50 cm. (B) Wild-type (left) and mutant (right) sibling from Mo17 x *Oy1-N1989/oy1*:Mo17 cross. Close-up view of the emerging tassel of mutant siblings (C) from panel A, and (D) from panel B. Distribution of (E) days to anthesis, (F) days to silking, and (G) Anthesis-silking interval (ASI) in the wild-type and mutant siblings in B73 and Mo17 x B73 (Mo17/B73) hybrid genetic backgrounds.

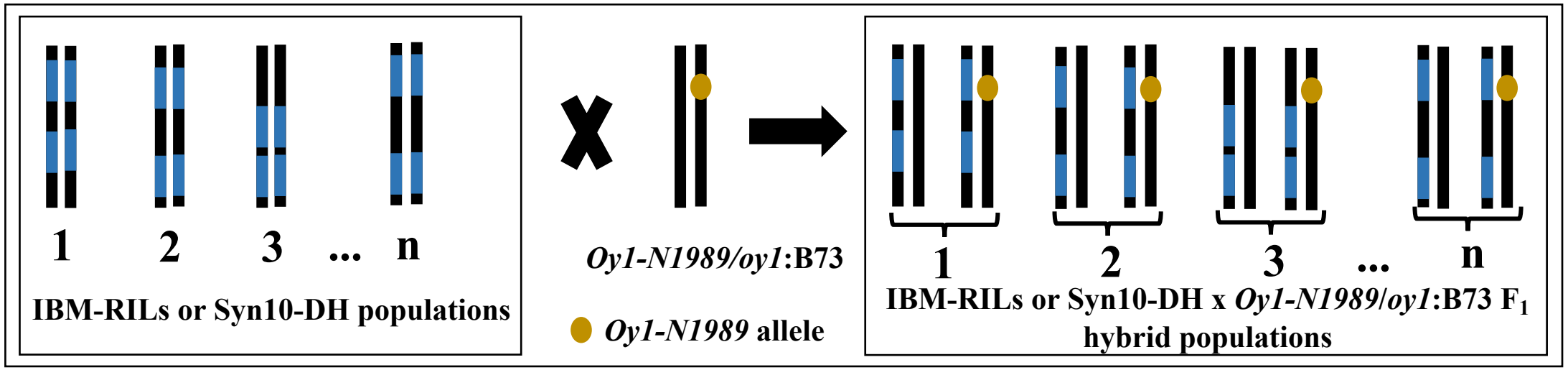

Figure 2. Crossing scheme to map *Oy1-N1989* enhancer/suppressor loci using IBM-RILs (n=216) and Syn10-DH (n=251) populations. Black and blue colors indicate B73 and Mo17 genotypes. Chromosome 10 of the heterozygous pollen parent *Oy1-N1989/+*:B73 is shown with a golden spot indicating *Oy1-N1989* mutant allele. The resulting F_1 progenies from these crosses are depicted here with state of chromosome 10 for each F_1 testcross showing segregation of wildtype and mutant (with the golden spot) siblings.

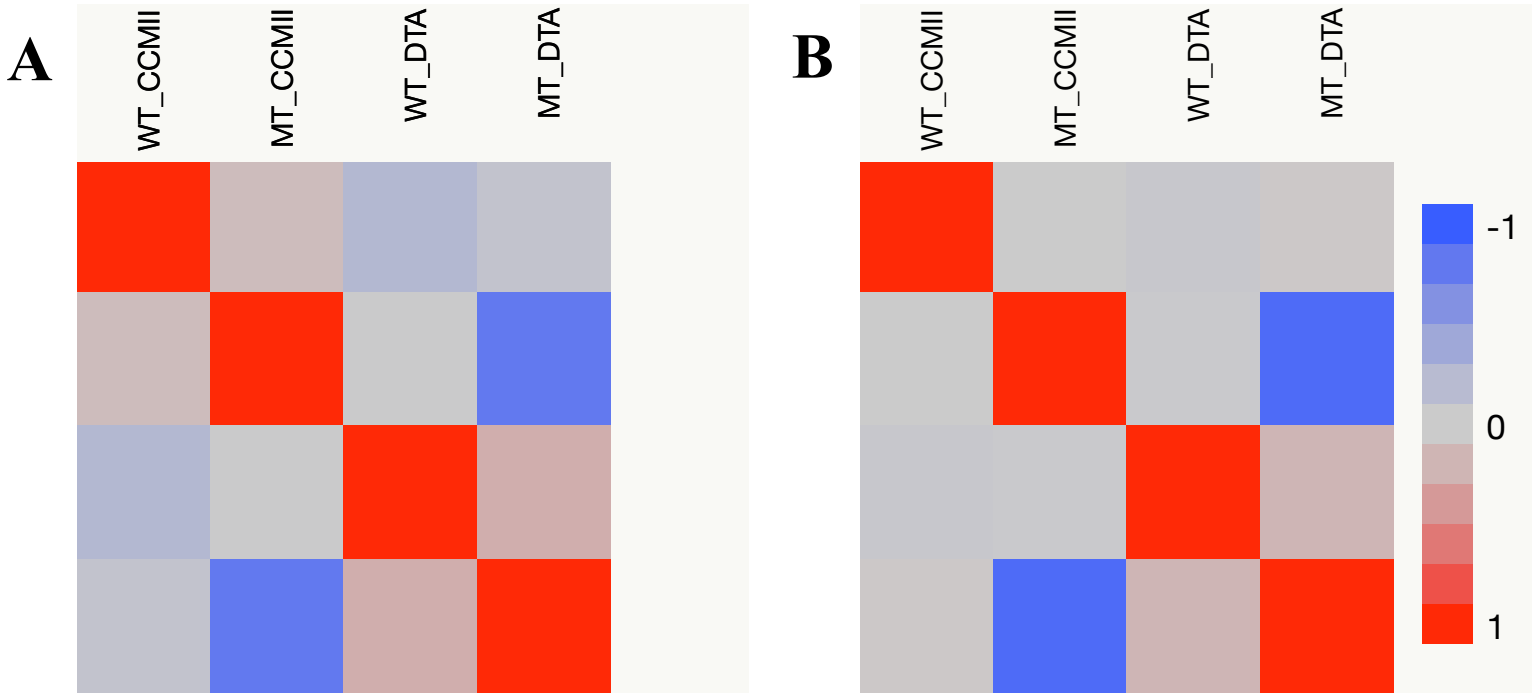

Figure 3. Pairwise correlation matrix between wildtype CCMII (WT_CCMII), mutant CCMII (MT_CCMII), wildtype days to anthesis (WT_DTA), and mutant days to anthesis (MT_DTA) in (A) IBM-RILs x *Oy1-N1989/oy1*:B73, and (B) Syn10-DH x *Oy1-N1989/oy1*:B73 F_1 test cross populations.

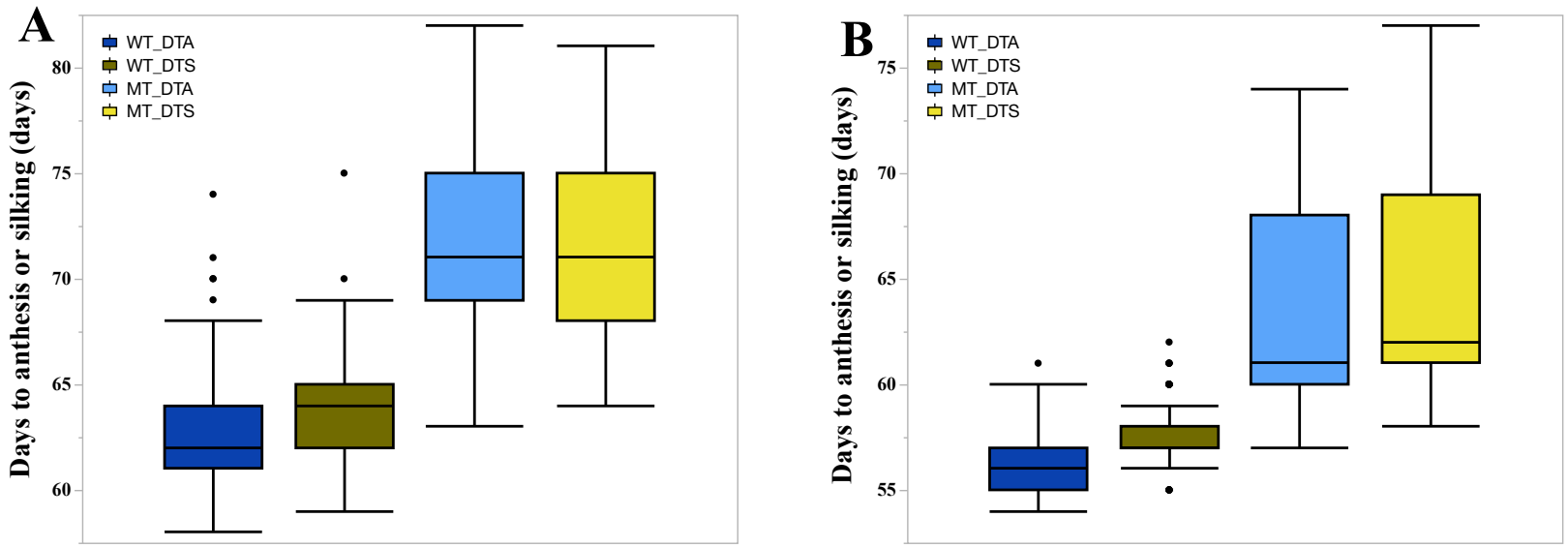

Figure 4. Distribution of days to flower (anthesis and silking) in the wildtype and mutant siblings in (A) IBM-RILs x *Oy1-N1989/oy1*:B73, and (B) Syn10-DH x *Oy1-N1989/oy1*:B73 F_1 test cross populations. Abbreviations: wildtype days to anthesis (WT_DTA), wildtype days to silking (WT_DTS), mutant days to anthesis (MT_DTA), and mutant days to silking (DTS).

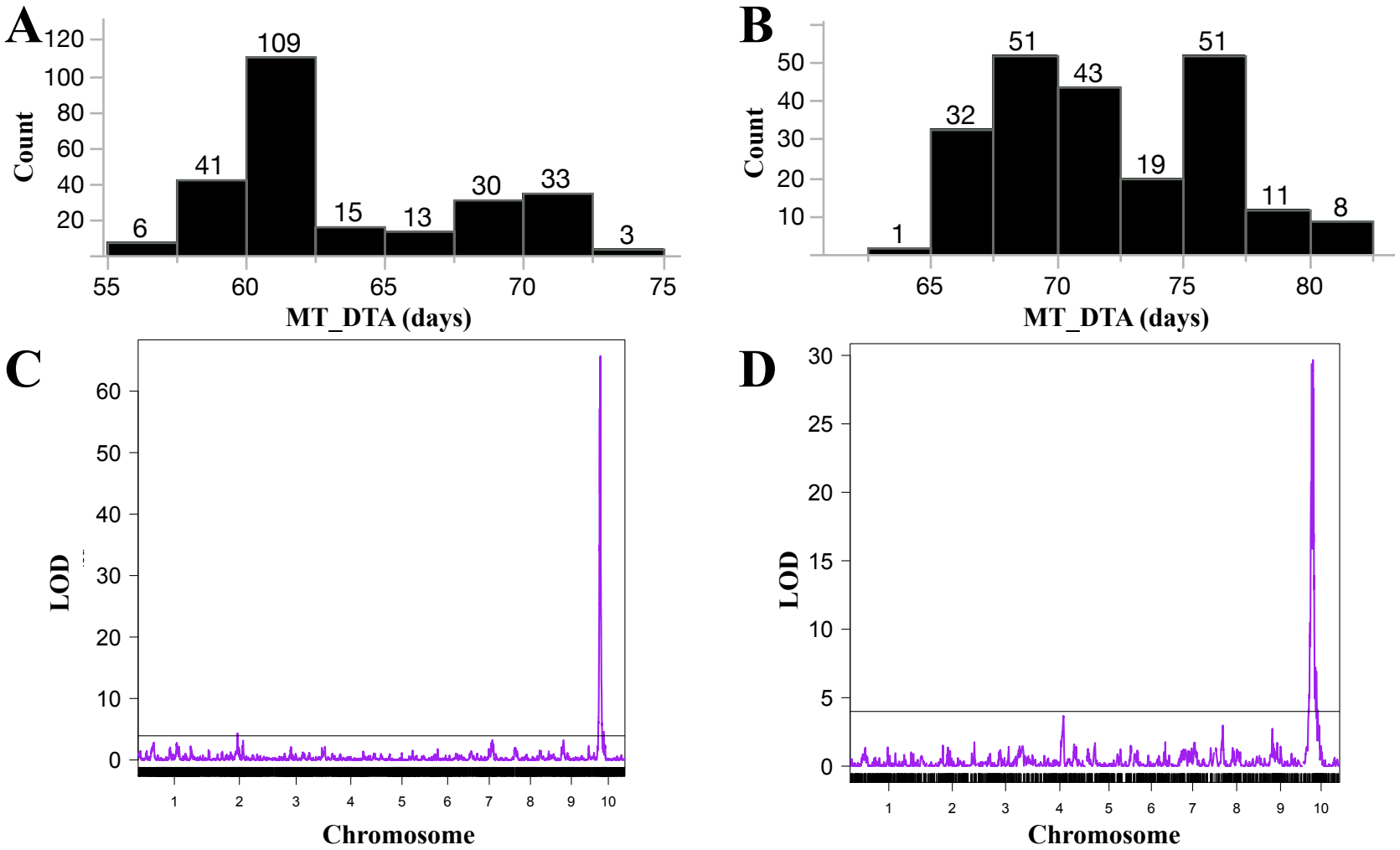

Figure 5. Distribution of days to 50% anthesis of the mutant siblings (MT_DTA) in (A) Syn10-DH x *Oy1-N1989/oy1*:B73, and (B) IBM-RILs x *Oy1-N1989/oy1*:B73 F_1 population. Genome wide QTL plot of MT_DTA in (C) Syn10-DH, and (D) IBM-RILs F_1 population. X-axis indicates the chromosome number and Y-axis indicates the logarithm of odds (LOD) of tested markers. Black horizontal bar indicates permutation testing based threshold for QTL detection.

Figure 6. Effect of *vey1* locus from B73 and Mo17 on flowering time in reciprocal isogenic backgrounds
(A) Delayed maturity of the heterozygous mutants in isogenic Mo17 (BC_7 generation) inbred background, compared to the wildtype siblings. Mutant and wildtype siblings in b030 (B73-like NIL with $vey1^{B73}$) shows early flowering while the isogenic B73 introgression of the $vey1^{Mo17}$ locus in b094 exhibits delayed flowering.
(B) Early maturity in the heterozygous mutant in m097 (Mo17-like NIL with $vey1^{B73}$) compared to the mutant in B73 x Mo17 F_1 hybrid background. Measuring stick on the left in both panels is 243 cm.

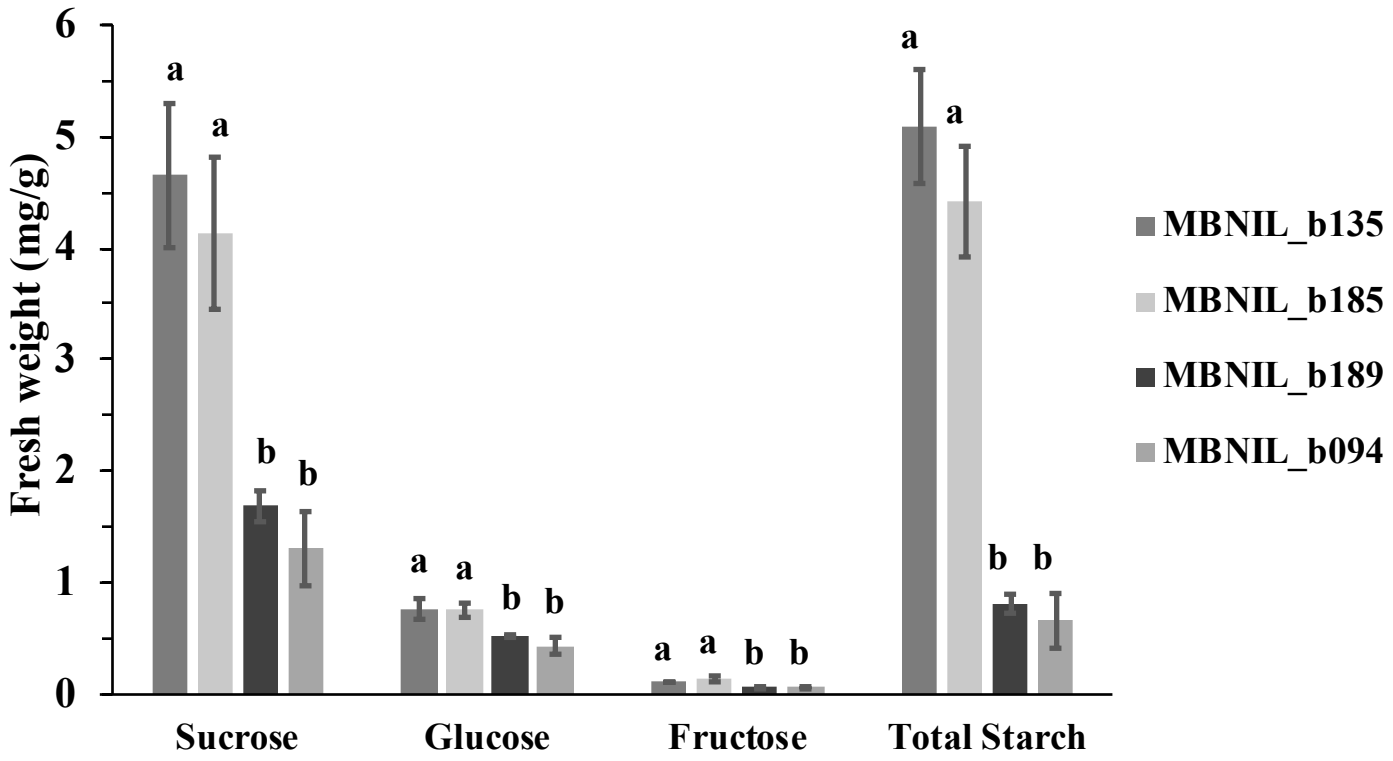

Figure 7. Effect of *vey1* on leaf soluble sugars and starch content in *Oy1-N1989/oy1* heterozygotes in the isogenic B73 NILs. NILs b135, and b185 have *vey1*^{B73} introgression, whereas b189, and b094 have *vey1*^{Mo17} introgression.

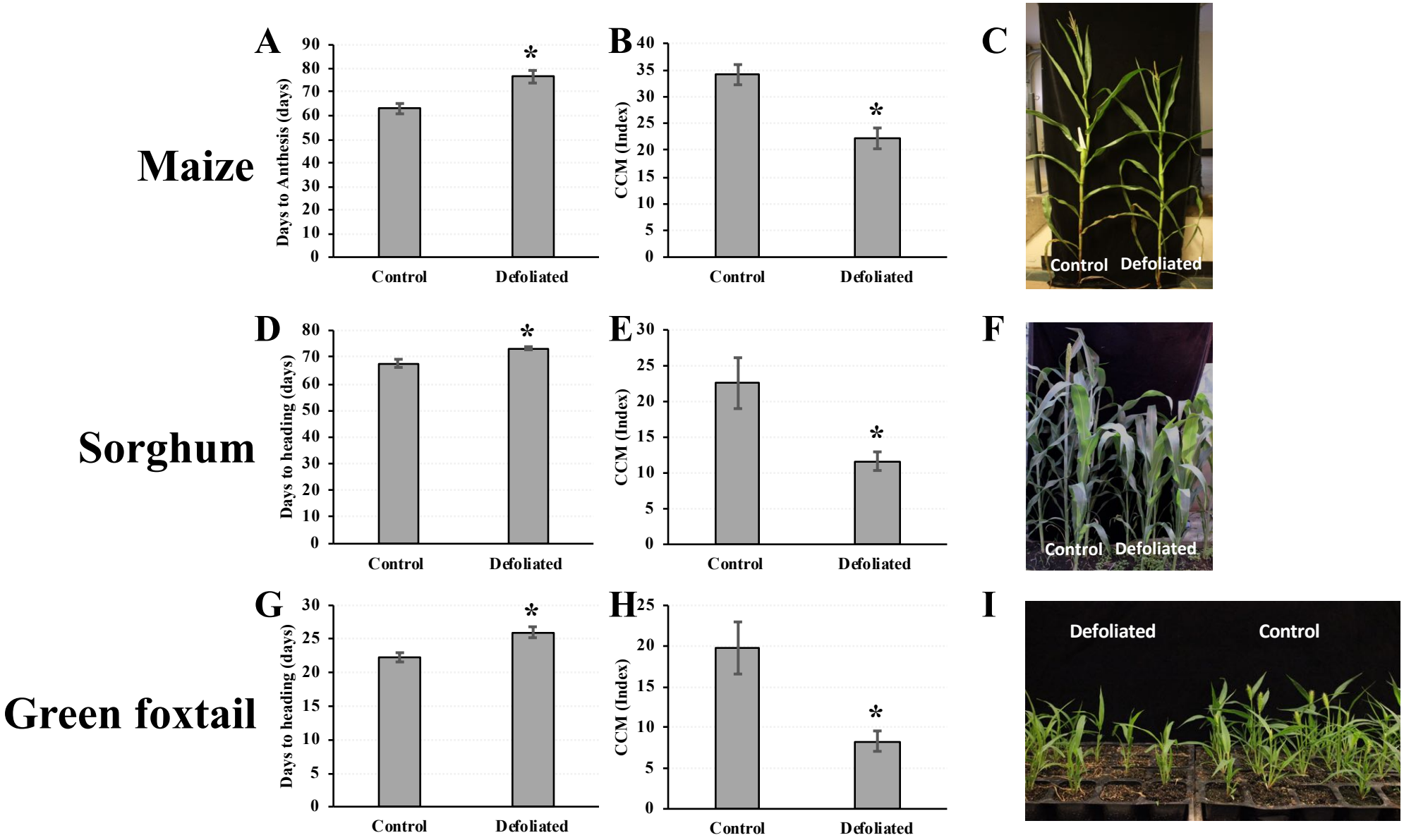

Figure 8. Effect of defoliation on flowering time and leaf color in (A-C) maize, (D-F) sorghum, and (G-I) green foxtail. Asterisk indicates significant difference between treatment means using student's t-test at $p<0.05$.

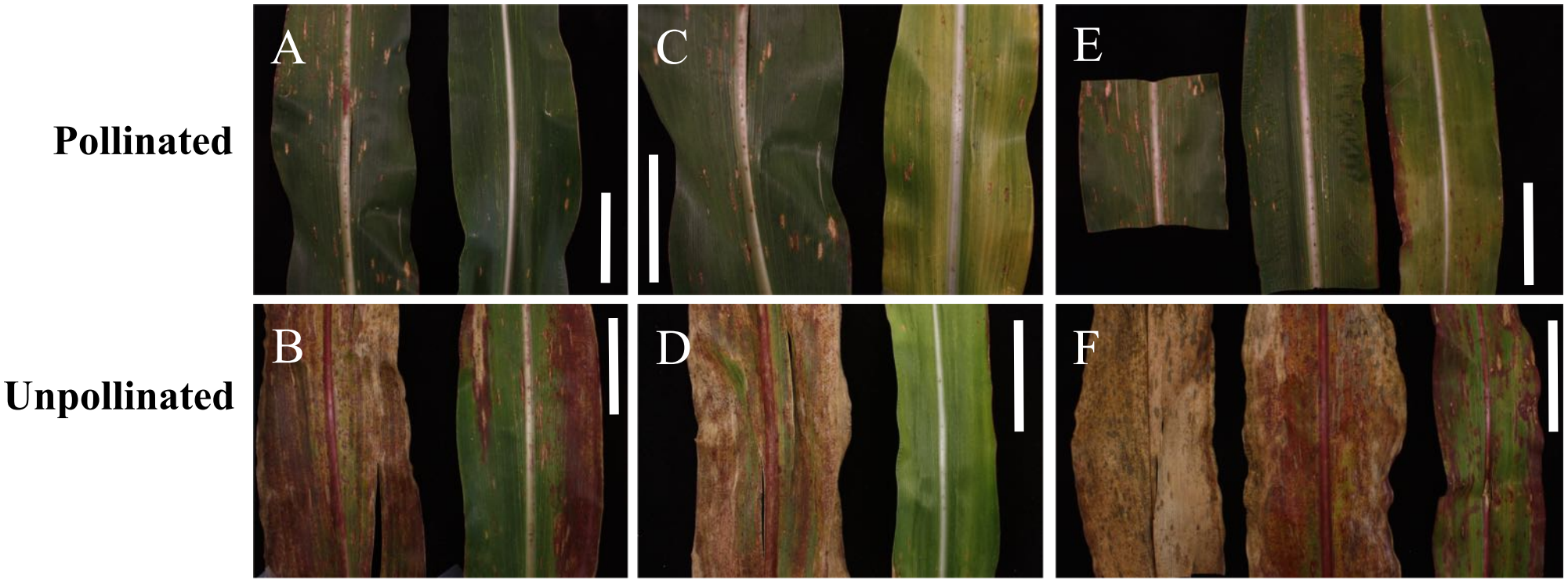

Figure 9. Effect of *vey1* on senescence induced by pollination prevention. Pictures of the representative primary ear leaf derived from plants at 30 and 40 days-after-anthesis (DAA) either with open pollinated (top panels: A, C, and E) or unpollinated (bottom panels: B, D, and F) ears. Representative primary ear leaf from (A-B) B73 wildtype (left) and mutant sibling (right) at 30DAA, (C-D) wildtype (left) and mutant (right) sibling from F_1 between B73-like NIL-b107 (with *vey1*^{Mo17} introgression) X *Oy1-N1989/oy1*:B73 at 30 DAA, (E-F) wildtype (B73-like NIL-b107), mutant B73-like NIL-b135 with *vey1*^{B73} (middle), and mutant B73-like NIL-b107 with *vey1*^{Mo17} (right) at 42 DAA. Scale bar in each figure is 6.35 cm.